MAGNETICALLY INDUCED BIOMAGNETIC FLUID MIXING – FEM MODEL

Al.M. Morega*, M. Morega* and S.C Faur

POLITEHNICA University of Bucharest
Department of Electrical Engineering
Bucharest-6, Romania
* IEEE Member

amm@iem.pub.ro

Abstract: Biomagnetic ferrofluids are subject to body forces when exposed to magnetic fields. This reaction, due to magnetization, may be used for mixing purposes in a variety of MEMS μ-TAS applications. In this paper we propose a static magnetic mixer: we report a numerical (finite element) experiment conducted on a biomagnetic ferrofluid confined to slim, planar rectangular cavity, and subject to an in-plane external variable magnetic field produced by DC current passing through traveling wires conveniently placed outside the cavity. The variable magnetic field produces dynamic body forces in the magnetized fluid that entrain the otherwise at rest biomagnetic fluid into a complex flow. The horizontal walls have different, imposed temperatures; this leads to a temperature dependent, non-uniform magnetization contributing to mixing flow enhancement. The action of the magnetic field and the convective process are observed also via flow visualization and through the skin friction coefficient and the heat transfer rate.

Introduction

Mixing of biomagnetic fluids is a critical issue in biological micro-scale lab-on-chip micro-total-analysis systems (μ-TAS MEMS), because of their small diffusivity. Active micro-mixers reach rapid and efficient mixing even in creeping flow. Supplementary, magnetically induced mixing may be added [1]-[4]. Drug targeting by magnetically controlled biomagnetic fluids is another area of intense research [10].

The Biofluid-Dynamics (BFD) models of biomagnetic fluids do not account for polarization, as for Magneto-Hydro-Dynamics (MHD): Lorentz's force here is much smaller than the magnetizing force because biomagntic fluids are magnetizable media whereas their electrical conductivity is very small [2], [5]. Therefore, magnetization rather than induced currents is the main phenomenon that occurs when biomagnetic fluids are exposed to magnetic fields.

In this paper we propose a static mixer and report the FEM study on the magnetically induced mixing of a biomagnetic fluid confined to a planar cavity, by an external magnetic field produced by DC currents orthogonal to the cavity plane (Fig.1). The top and bottom walls may be set to different temperatures, leading to temperature dependent magnetization of the biomagnetic medium [7], [8].

The mathematical model we develop is solved numerically by FEM FEMLAB multiphysics package [14]. The results show the effect of the magnetic field on the non-isothermal flow and suggest the potential of this mixing principle.

Mathematical Model

The mathematical model is based on several simplifying assumptions presented next.

The biomagnetic fluid is viscous, linear, Newtonian, with constant properties. As the channels and cavities filled with the working fluid in μ-TAS devices are typically planar and the dimensions in the direction orthogonal to the flow (height) are much smaller than those in-plane due to the intrinsic property of thin-film process such as spin-coating, evaporation, and chemical vapor deposition [1]-[4], the flow is assumed 2D, incompressible and laminar. The cavity walls are no-slip, consistent with the viscous flow regime.

The magnetic field is produced by DC currents, which pass through wires that are orthogonal to the cavity plane. The wires are in oscillatory motion with respect to the cavity. This relative motion (wires-cavity) translates into a variable magnetic field within the fluid region. We decided to use this model of source for the magnetic field because of its analytic closed form. In this arrangement, the magnetic field is in a sort of "peristaltic" motion with respect to the working fluid. From a practical point of view, other sources may be considered [4], [8].

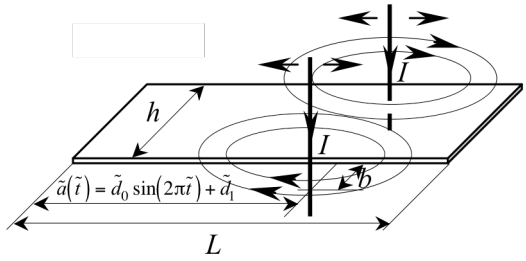

Figure 1: Static magnetic mixer – working principle

Figure 1 shows the sketch of the computational domain. The cavity height is h = 10μm, and L = 140μm

ISSN: 1727-1983

is its length. The horizontal (long) walls have imposed temperatures, T_u = 50ºC and T_w = 10ºC respectively and the vertical (short) walls are adiabatic [8], [11], [12].

In the absence of a variable magnetic field there is no motion, except for natural convection. However, we recognize that this effect is negligible small for the thermal conditions assumed here. The mathematical model is then [8], [9], [11]-[13]

Mass conservation

$$\frac{\partial u}{\partial x}+\frac{\partial v}{\partial y}=0, \tag{1}$$

Momentum balance (*Navier-Stokes*)

$$\begin{aligned}\rho\left(\frac{\partial u}{\partial t}+u\frac{\partial u}{\partial x}+v\frac{\partial u}{\partial y}\right)&=-\frac{\partial p}{\partial x}+\mu_0 M\frac{\partial H}{\partial x}+\mu\left(\frac{\partial^2 u}{\partial x^2}+\frac{\partial^2 u}{\partial y^2}\right),\\ \rho\left(\frac{\partial v}{\partial t}+u\frac{\partial v}{\partial x}+v\frac{\partial v}{\partial y}\right)&=-\frac{\partial p}{\partial y}+\mu_0 M\frac{\partial H}{\partial y}+\mu\left(\frac{\partial^2 v}{\partial x^2}+\frac{\partial^2 v}{\partial y^2}\right),\end{aligned} \tag{2}$$

Energy balance (accounting for viscous dissipation)

$$\begin{aligned}\rho c_p\left(\frac{\partial T}{\partial t}+u\frac{\partial T}{\partial x}+v\frac{\partial T}{\partial y}\right)&=-\mu_0 T\frac{\partial M}{\partial T}\left(u\frac{\partial H}{\partial x}+v\frac{\partial H}{\partial y}\right)+\\ +k\left(\frac{\partial^2 T}{\partial x^2}+\frac{\partial^2 T}{\partial y^2}\right)&+\mu\left[2\left(\frac{\partial u}{\partial x}\right)^2+2\left(\frac{\partial v}{\partial y}\right)^2+\left(\frac{\partial v}{\partial x}+\frac{\partial u}{\partial y}\right)^2\right],\end{aligned} \tag{3}$$

and the *magnetization (constitutive) law*

$$M=KH(T_c-T). \tag{4}$$

Here x, y are Cartesian coordinates; u, v are the velocity components; T is temperature; $T_c = 770^\circ\mathrm{C}$ is the Curie temperature for Iron; M is the magnetization, μ_0 is the magnetic permeability of vacuum. The biomagnetic fluid properties are [8]: thermal conductivity $k = 2.2\times10^{-3}\,\mathrm{J/m\cdot s\cdot K}$, mass density $\rho = 1050\,\mathrm{kg/m^3}$, specific heat $c_p = 14.65\,\mathrm{J/kg\cdot K}$, dynamic viscosity $\mu = 3.2\times10^{-3}\,\mathrm{kg/m\cdot s}$. The magnetic field strength of a filamentary current I has the closed form [11]

$$H=I/(2\pi r),\quad r=\sqrt{(x-a)^2+(y-b)^2}. \tag{5}$$

For $b \geq 0$ (i.e., at a location inside the cavity) eq. (5) gives accurate, physical values for the magnetic field strength.

Equation (2) shows that the magnetic body force term depends on the magnetization of the medium and on the magnetic field gradient. The magnetic field source we use (filamentary current) provides for the field gradient, whereas magnetization is the biomagnetic fluid contribution.

The non-dimensional model is

Mass conservation

$$\frac{\partial \tilde u}{\partial \tilde x}+\frac{\partial \tilde v}{\partial \tilde y}=0, \tag{6}$$

Momentum balance

$$\begin{aligned}&\frac{\partial \tilde u}{\partial \tilde t}+\tilde u\frac{\partial \tilde u}{\partial \tilde x}+\tilde v\frac{\partial \tilde u}{\partial \tilde y}=\\ &-\frac{\partial \tilde p}{\partial \tilde x}+\mathrm{M_n}\tilde H\frac{\partial \tilde H}{\partial \tilde x}(\theta-\theta_c)+\frac{1}{\mathrm{Re}}\left(\frac{\partial^2 \tilde u}{\partial \tilde x^2}+\frac{\partial^2 \tilde u}{\partial \tilde y^2}\right),\\ &\frac{\partial \tilde v}{\partial \tilde t}+\tilde u\frac{\partial \tilde v}{\partial \tilde x}+\tilde v\frac{\partial \tilde v}{\partial \tilde y}=\\ &-\frac{\partial \tilde p}{\partial \tilde y}+\mathrm{M_n}\tilde H\frac{\partial \tilde H}{\partial \tilde y}(\theta-\theta_c)+\frac{1}{\mathrm{Re}}\left(\frac{\partial^2 \tilde v}{\partial \tilde x^2}+\frac{\partial^2 \tilde v}{\partial \tilde y^2}\right),\end{aligned} \tag{7}$$

Energy balance

$$\begin{aligned}&\mathrm{Re\,Pr}\left(\frac{\partial \theta}{\partial \tilde t}+\tilde u\frac{\partial \theta}{\partial \tilde x}+\tilde v\frac{\partial \theta}{\partial \tilde y}\right)=\\ &-\mathrm{Ec\,Pr\,Mn\,Re}\,\tilde H(\theta-\varepsilon)\left(\tilde u\frac{\partial \tilde H}{\partial \tilde x}+\tilde v\frac{\partial \tilde H}{\partial \tilde y}\right)+\\ &+\left(\frac{\partial^2 \theta}{\partial \tilde x^2}+\frac{\partial^2 \theta}{\partial \tilde y^2}\right)+\mathrm{Pr\,Ec}\left[2\left(\frac{\partial \tilde u}{\partial \tilde x}\right)^2+2\left(\frac{\partial \tilde v}{\partial \tilde y}\right)^2+\left(\frac{\partial \tilde v}{\partial \tilde x}\frac{\partial \tilde u}{\partial \tilde y}\right)^2\right],\end{aligned} \tag{8}$$

Magnetization law

$$\tilde M=\mathrm{Mn}(\theta-\varepsilon), \tag{9}$$

where $(\tilde x,\tilde y)=(x,y)/h$, $(\tilde u,\tilde v)=(u,v)/U_r$, $\tilde H = H/H_0$, $\theta=(T_u-T)/(T_u-T_W)$, $p=\tilde p/(\rho U_r^2)$. The groups are: Reynolds $\mathrm{Re}=h\rho U_r/\mu$, Prandtl $\mathrm{Pr}=c_p\mu/k\to20$, Eckert $\mathrm{Ec}=U_r^2/[c_p(T_u-T_w)]\to2.536\times10^{-7}$, magnetic $\mathrm{Mn}=\mu_0 H_0^2 K(T_u-T_w)/(\rho U_r^2)$, and $\varepsilon=T_u/(T_u-T_w)\to8$. H_0 is a reference value for the magnetic field strength produced by a filamentary DC current – typically, the magnetizing field 60A/m.

The proposed "peristaltic" mixing by magnetic field is an alternative to the forced flow option [11], [12], therefore we kept the goal of same Re number of the flow (1...40), and used the same reference velocity (U_r = 1.22×10^{-2}m/s) that proved mixing efficiency. In this setup, the frequency of the oscillatory motion varies (increases) with Re. For instance, at Re = 40 the period of oscillation is $T_0 = L/U_r = 1.15\times10^{-2}\,\mathrm{s}$. The instantaneous position of the wire is given by $\tilde a=\tilde d_1\sin(2\pi\tilde t)+\tilde d_0$, $\tilde b=0.4$, where $\tilde d_1 = L/h$.

The mathematical model was implemented and solved in FEMLAB that uses the Galerkin finite element formalism [14]. The mesh is unstructured, triangular, Delaunay. Roughly, 16000-18000 elements were needed to get mesh independent solutions. We selected Lagrange quadratic elements, the P_1-P_2 formulation. The results reported here were obtained by using the transient GMRES solver with a LU preconditioner. The drop tolerance was set 10^{-5}.

Results and Discussion

Figure 2 shows several time instances of the mixing process for $\tilde t\in(4,5]$: the magnetic field strength

ISSN: 1727-1983

(contours), the flow field (streamlines and vectors), and the thermal field (grey map) when the wire by the bottom wall is powered. Here, $\tilde{d}_1 = 5, \tilde{d}_0 = 2.5$. Two recirculation cells are competing in an oscillatory mixing process as the magnetic field follows its traveling source.

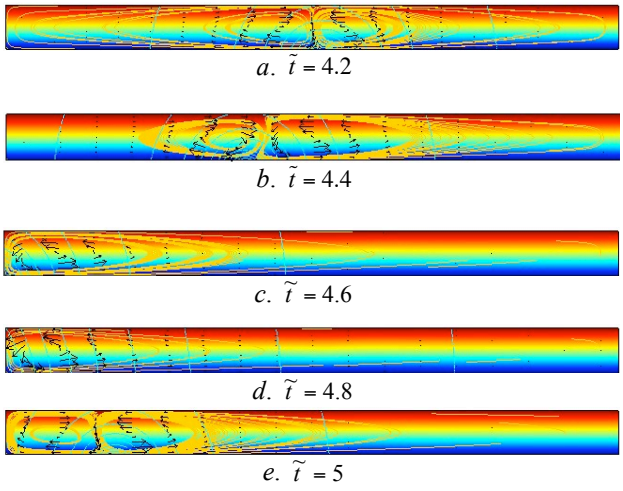

a. $\tilde{t} = 4.2$

b. $\tilde{t} = 4.4$

c. $\tilde{t} = 4.6$

d. $\tilde{t} = 4.8$

e. $\tilde{t} = 5$

Figure 2: Magnetic mixing at Re = 1, Mn = 20 – magnetic field produced by the bottom current.

As expected for an inertial, viscous flow, the separation interface between the rolls changes its inclination as the fluid is entrained from the bottom in one direction or the other. The flow seems complex enough to be used for mixing purposes (e.g., in μ–TAS).

Figure 3,*a* displays the skin friction coefficient, $\tilde{C}_f = (1/\mathrm{Re})(\partial\tilde{u}/\partial\tilde{y})\big|_{\tilde{y}=0,1}$, at the bottom wall, where the most vigorous entrainment occurs. The high frequency content suggests that the laminar regime is at its limits, and turbulence would eventually set in at the bottom wall when further increasing the Re number (i.e., the frequency of oscillation for the traveling wire).

The local Nusselt number, $\mathrm{Nu} = \partial\theta/\partial\tilde{y}\big|_{\tilde{y}=0,1}$, at the bottom wall (Fig.3,b) indicates that at $\tilde{t} = 5$ the transient regime persists after five periods. Apparently, the Nu profile does not change significantly, indicating that heat transfer occurs mainly by conduction.

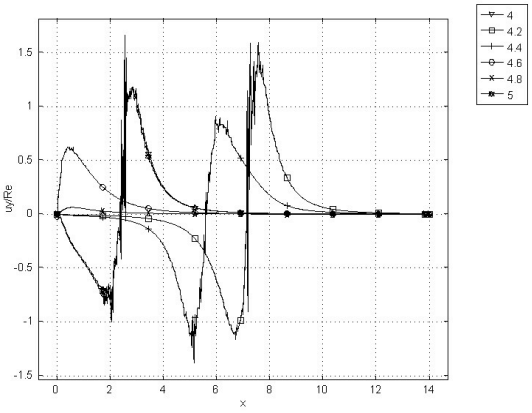

a. Skin friction coefficient

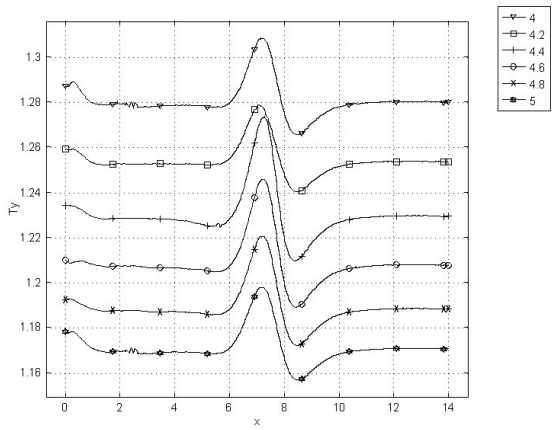

b. Local Nusselt number

Figure 3: Mixing flow at Re = 1, Mn = 20 – magnetic field produced by the current at the bottom wall.

The two-sided lobe in the middle indicates enhancement and reduction in heat transfer, which on average (in space) is at the cavity level. Note that the right limit of the wire excursion is $\tilde{x} = 7.5$.

Next, we present the results for the flow at Re = 1 and Mn = 20, when both wires are powered, and the currents have the same orientation (Fig.1). Here, $\tilde{d}_1 = 5, \tilde{d}_0 = 7$. The magnetic field spectrum is now symmetric with respect to the long symmetry axis (Fig.4,a), which – at mild temperature gradients – explains the almost symmetric flow. This suggests that the temperature gradient in the fluid is small enough such that its influence on the fluid magnetization – that might destroy the flow symmetry – is not that important. In this case too, two cells are competing into filling the cavity. However, unlike the previous setup, in this case both cells always exist.

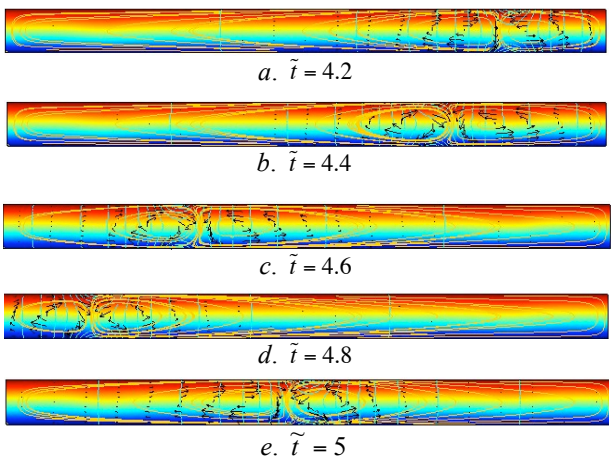

a. $\tilde{t} = 4.2$

b. $\tilde{t} = 4.4$

c. $\tilde{t} = 4.6$

d. $\tilde{t} = 4.8$

e. $\tilde{t} = 5$

Figure 4: The peristaltic mixing flow for Re = 1, Mn = 20. The magnetic field is sourced by both currents.

The high frequency content in the $\tilde{C}_f$ signal recorded in the previous case are smoothed out to a large extent here (Fig.5,a), but turbulence would set in for higher Re number (i.e., the frequency of oscillation for the traveling wire). The local Nu number at the

ISSN: 1727-1983

bottom wall (Fig.5,b) shows that after five periods the quasi-steady regime is not reached yet. The profile does not change significantly in time, which means that conduction heat transfer prevails.

The Nu master profile exhibits two, one-sided lobes, by the vertical walls. The higher temperature gradients here indicate more vigorous heat transfer.

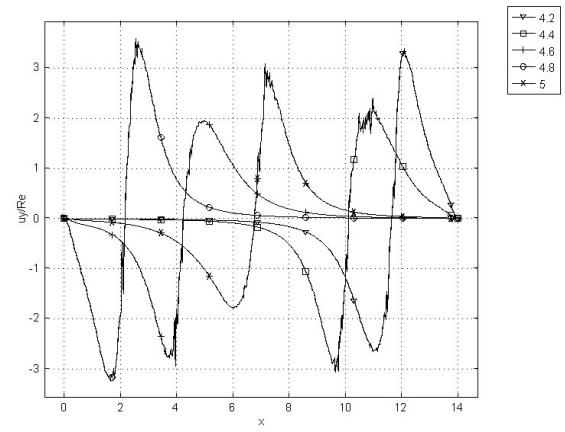

a. Skin friction coefficient

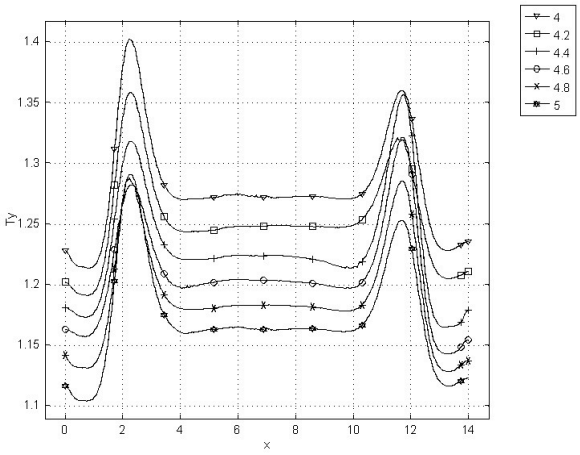

b. Local Nusselt number

Figure 5: Skin friction coefficient and Nusselt number at the bottom wall for Re = 1, Mn = 20.

The simulation results for Re = 40 and Mn = 20 are presented elsewhere [12].

Next, we briefly show the underlying features of the mixing flow for two-sided magnetic mixing: Figure 6 depicts several instances of the flow, temperature field and the magnetic field (the wire at the bottom wall is powered) during the fifth period of oscillation. Two cells, whose interface is entrained by the current, and a third, residual cell, are seen. Apparently, the flow is almost uniform, at the upper wall temperature (see Fig. 2 and 4, at Re = 1).

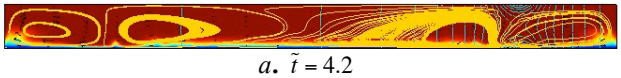

a. $\tilde{t} = 4.2$

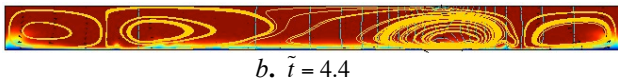

b. $\tilde{t} = 4.4$

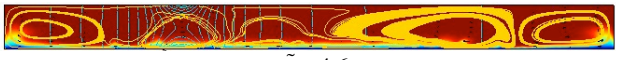

c. $\tilde{t} = 4.6$

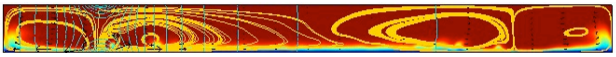

d. $\tilde{t} = 4.8$

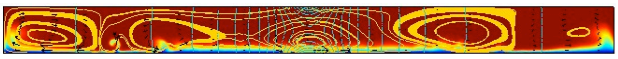

e. $\tilde{t} = 5$

Figure 6: The flow for Re = 40, Mn = 20. The current source is by the bottom wall.

Figure 7,a displays the skin friction coefficient at the bottom wall. The local Nu number profile (Fig. 7,b) indicates that heat transfer is still mainly by conduction. The high frequency content in the signal for the left side of the cavity confirms that this area will first experience the turbulence, should Re be further increased.

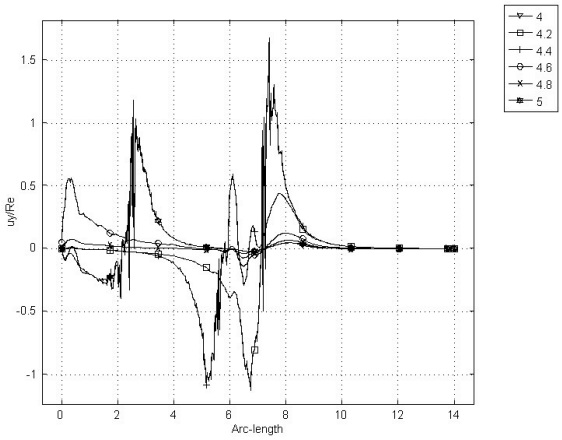

a. Skin friction coefficient

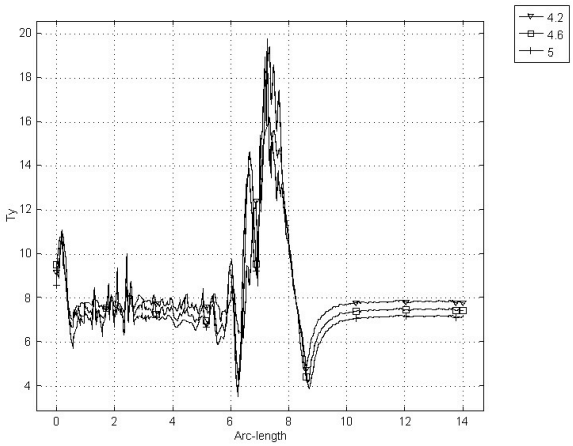

b. Local Nusselt number

Figure 7: Skin friction coefficient and Nusselt number at the bottom wall for Re = 40, Mn = 20.

The high frequency content is more important, but turbulence is not yet prevailing. Comparing Fig. 7 and Fig.5 we may conjecture that at $\tilde{t} = 5$ heat transfer approaches a steady state regime, and the flow (Fig. 7,a) exhibits a quasi-steady state motion.

Finally, Fig. 8 shows a detail of the mixing flow (yellow streamlines and black arrows) for a particular

ISSN: 1727-1983

time moment in the case when the magnetic field is produced by both currents: the magnetic field strength (dark contour lines), and the temperature field (colored surface map) for Re = 1 and 40 when Mn = 20. In this setup, after five periods of oscillation the temperature field in the flow is almost isothermal (at the upper wall temperature) for Re = 40, whereas for Re = 1 the fluid is uniformly thermally stratified, indicating that at Re =1 a larger part of the fluid core is at lower temperature, hence its magnetization is more important.

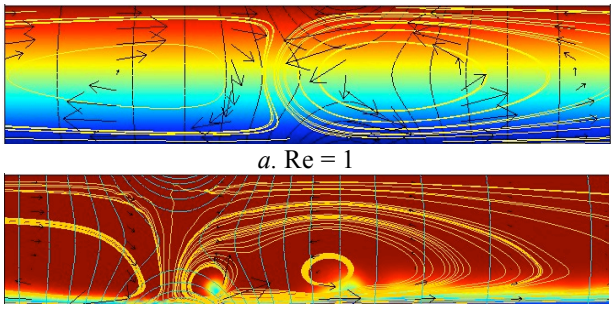

a. Re = 1

b. Re = 40

Figure 8: Details of the mixing flow for Mn = 20.

Although higher magnetization suggests a more vigorous mixing, more important to the success of magnetic peristaltic mixing is the frequency of oscillation, which translates into the Re number of the flow – as indicated by the more complex flow structure, and higher velocities in Fig. 8,b.

Conclusions

In this paper we present a magnetic, peristaltic mixing concept for biomagnetic fluids, and we report the numerical study on the associated flow for Re = 1, 40, and Mn = 20. The main conclusions are:

A variable magnetic field may produce a peristaltic mixing flow, characterized by recirculation; depending on the magnetic field, its gradient and the frequency of oscillation, one or more rolls may exist.

At higher Re numbers the flow bifurcates into more cells: for example at Re = 40 there are five distinguishable rolls.

At higher Re numbers the flow may become turbulent, as suggested by the friction coefficient and the local Nu number at the bottom wall.

Heat transfer is mainly by conduction, as suggested by the Nu diagrams; its stratification is perturbed by the magnetic field action. However, the higher the frequency of oscillation (hence, Re number) the closer the flow to isothermal, at the top wall temperature. It approaches steady state (mainly conduction); it is less so for the flow, which approaches a quasi-steady state.

Magnetic peristaltic mixing of a biomagnetic fluid confined to a no-slip wall cavity is an alternative to the conventional, forced flow procedure.

References

[1] SUZUKI, H., KASAGI, N., HO, C.M. (2003): 'Chaotic Mixing of Magnetic Beads in Micro Cell Separator", Proc. 3rd Int. Symp. Turbulence and Shear Flow Phenomena, Sendai, p. 817-822.

[2] HAIK Y., PAI V., CHEN C. J. (1999): 'Development of magnetic device for cell separation', *J. of Magnetism and Magnetic Materials*, **194**,p.254-261

[3] PLAVINS J., LAUVA M. (1993): 'Study of Colloidal Magnetite Binding Erythrocytes: Prospects for Cell Separation', *J. of Magnetism and Magnetic Materials*, **122**, p. 349-353

[4] SUZUKI H. (2003): 'Development of a Chaotic Micro-Mixer Using Magnetic Beads', PD Thesis, UCLA, USA

[5] ROSENSWEIG R. E. (1985): 'Ferrohydrodynamics', (Dover Publications, Mineola, New York)

[6] PAULING L., CORYELL C. D., (1936): 'The magnetic Properties and Structure of Hemoglobin, Oxyhemoglobin and Carbonmonoxy Hemoglobin', Proc. Nat. Acad. Sci., USA, **22**, p.210-216

[7] ANDERSSON H. I., VALNES O. A. (1998): 'Flow of a heated ferrofluid over a stretching sheet in the presence of a magnetic dipole', *Acta Mechanica*, **128**, p. 39-47

[8] TZIRTZILAKIS E. E., KAFOUSSIAS B. G., HATZIKONSTANTINOU P. M. (2002): 'Biomagnetic fluid flow in a rectangular duct', 4th GRCAM Congress on Computational Mechanics, Patras, Greece, June 27-29, 2002

[9] HAIK Y., CHEN J. C., PAI V. M. (1996): 'Development of bio-magnetic fluid dynamics', in S. H. WINOTO, Y. T. CHEW (Ed): 'Proc. IXth International Symposium on Transport Properties in Thermal Fluids Engineering', Singapore, June 25-28, p. 121-126

[10] STRAUSS D. (2005): 'Magnetic drug targeting in cancer therapy', Internet site address: http://www.comsol.com/showroom

[11] FAUR S., MOREGA AL.M. (2004): 'A FEM analysis of biomagnetic fluid flow in a rectangular duct under the influence of a magnetic field', 4th European Symposium on Biomedical Engineering, Univ. of Patras, Greece, June 25-27, 2004

[12] MOREGA AL. M., FAUR S., 'A numerical model for the blood flow – magnetic field interaction', Mathematical Modeling of Environmental and Life Sciences Problems, 3rd Workshop, Constanta, Romania, 27-30 May, 2004

[13] MOREGA AL. M., MOREGA M. (2005): 'A FEM analysis of Magnetically induced biomagnetic fluid mixing', Rev. Roum. Scie. Tech. Electrotechnique et Energetique, to appear

[14] FEMLAB, v.31*i*, COMSOL AB, Sweden, 2005